Solute Transport in Unsaturated Soil: Experimental Design, Parameter Estimation, and Model Discrimination

T. R. Ellsworth,* P. J. Shouse, T. H Skaggs, J. A. Jobes, and J. Fargerlund

ABSTRACT

The objectives of this study were to: (i) examine the efficacy of two sampling techniques for characterizing solute transport under steady-state water flow, (ii) study the variation in transport model parameters with increasing depth of solute leaching, and (iii) perform model discrimination to examine the transport process operative within a field plot. Bromide, NO_3^-, and Cl- were applied sequentially to a plot instrumented with two sets of 12 solution samplers located at depths of 0.25 and 0.65 m. At the conclusion of the experiment we destructively sampled the entire 2.0 by 2.0 m plot to a depth of 2.0 m. Mass recovery by the solution samplers ranged from 63 to 83% for the three tracers, and recovery by soil excavation ranged from 96 to 105%. The mean solute velocity estimated with the solution sampler data was significantly less than that determined by soil excavation. Mean solute velocity determined from soil excavation implied an effective transport volume equal to 0.828, (where θ_v is volumetric water content) for the three tracers. Solution samplers and soil excavation provided similar measures of vertical dispersion. Both sampling methods revealed a scale-dependent dispersion process in which the dispersivity increased linearly with mean residence time. The depth profiles for all three solutes were accurately described with a stochastic convective lognormal transfer function model (CLT) using the applied mass and two constant parameters (estimated from simultaneous fitting to the depth profiles).

ENVIRONMENTALLY HARMFUL anthropogenic chemicals frequently enter natural ecosystems, either by accident or by accepted management practices. Increased public awareness and concern has led to an expanded regulatory effort aimed at providing accurate assessments of the environmental fate of these compounds under a wide variety of management and climatic conditions. To this end, numerous environmental fate and transport models have been developed (van Genuchten and Shouse, 1989). One principal limiting factor to model development and discrimination is the lack of experimental research that examines transport mechanisms of chemicals through unsaturated field soils (Dagan, 1986; Jury and Flühler, 1992).

As noted by Gelhar et al. (1992), considerable experimental evidence exists that supports the theory of a scale-dependent dispersion process in aquifers (Gelhar and Axness, 1983; Dagan, 1984, 1987; Sposito and Barry, 1987). This is typically shown by fitting the V (mean solute velocity) and D (dispersion coefficient) CDE parameters to tracer data sampled sequentially in time and then plotting the dispersivity, a (the ratio D/V), against time of sampling (and/or mean travel

distance), with a generally observed to increase with either of these. Theoretically, for unsaturated soil-water flow systems, scale-dependent dispersion would apply when the dominant mechanism of effective dispersion is the variation in local pore-water velocity arising from variability in the hydraulic conductivity of the soil (Russo, 1991; Russo and Dagan, 1991; Beven et al., 1993).

No clear consensus exists, however, for scale-dependent dispersion in solute transport experiments through unsaturated field soils (Porro et al, 1993; Bevan et al, 1993; Jury and Fliihler, 1992). The dispersion coefficient, **D,** has been found to vary with depth in many ways: linear increase, nonlinear increase, constant, decrease, and erratic fluctuations. In a laboratory experiment, Kahn and Jury (1990) measured the outflow concentrations of tracers from repacked and undisturbed soil columns of various lengths, flow rates, and column diameters. They found that for the repacked columns, **D** was constant. For undisturbed columns, **D** was constant for only the lowest flow rate, and at the higher flow rates **D** increased with column length. One of two large-scale (6-m-deep and 0.95m-diam.) column studies of solute transport through a homogeneous soil in New Mexico found that **D** tended to increase to a depth of 4.0 m (Wierenga and van Genuchten, 1989). However, **D** had an erratic relationship with depth in the second column study (Porro et al., 1993). Jaynes and Rice (1993) monitored solute transport in a heterogenous profile with solution samplers at multiple depths on a 37-m^2 field plot under both drip and ponded irrigation water applications. Although quite erratic, a slight decrease in dispersivity with depth was observed under both water application methods. In a layered soil, Porro et al. (1993) showed that **D** was independent of depth as long as the layer thickness was small relative to the observation scale. At the field scale, Butters and Jury (1989) found that **D** increased to a depth of 13 m, except for a 40% decrease between 3.0 and 4.5 m. They attributed the temporary decrease to the influence of an increase in silt content between depths of 3 .0 and 4.7 m. A series of studies of solute transport on a loamy sand soil (Hamlen and Kachanoski, 1992; van Wesenbeeck, 1993) in Canada used solution samplers along transects to monitor steady-flow solute transport at different fluxes. They found that the transect-scale travel time variance increased approximately as the square of the mean travel time, at least to a depth of 0.4 m, indicating that **D** increased linearly with travel time.

In contrast, a constant **D** was found by Roth et al.

T.R. Ellsworth, Dep. of Natural Resources and Environmental Sciences, Univ. of Illinois, 1102 S. Goodwin Ave., Urbana, IL 61801; P.J. Shouse, J.A. Jobes, and J. Fargerlund, USDA-ARS, U.S. Salinity Lab., 450 Big Springs Rd., Riverside, CA 92507; and T.H. Skaggs, Dep. of Environmental Engineering, Centre for Water Research, Univ. of Western Australia, Nedlands, WA 6907, Australia. Received 27 Jan. 1995. *Corresponding author (ellswort@uiuc.edu).

Abbreviations: CLT, convective lognormal transfer function; Cl. confidence interval; pdf, probability density function; CDE, convection-dispersion equation; BTC, breakthrough curve; NAW, net applied water; MLE. maximum likelihood estimates; SSQ, least squares regression; **MM,** method of moments; RMSE, root mean square error.

(1991). Chloride movement was monitored with 110 solution samplers in a soil that was extremely heterogeneous in the vertical direction. The Cl- pulse split, with 58% of the mass at the end of the study moving by preferential flow and the remainder moving more slowly through the matrix. Roth et al. (1991) evaluated the field-average longitudinal dispersion after the mass balance had been corrected for preferential flow. The dispersion of the Cl- pulse in the matrix was described accurately by the CDE with D constant, a remarkable result for such a heterogeneous profile.

Characterization of solute transport in the natural environment has proven to be a difficult task because of temporal and spatial variability of soil transport properties. In an often-cited study, Biggar and Nielsen (1976) concluded that at least 1000 samples would be needed to estimate the true mean solute velocity within $\pm 10\%$ on a 150-ha field. More recently, Adams and Gelhar (1992) presented findings from a natural gradient tracer test in Mississippi. In their experiment, despite a massive array of multilevel solution samplers, Br - mass recovery ranged between 45 and 300 % . They attributed the large variation in mass recovery to an interplay between the spatial variability in hydraulic conductivity and their sampling methodology.

Two recent studies in a 0.64-ha field show the interaction between spatial variability and experimental methodology . Butters and Jury (1989) used solution samplers to monitor solute transport under steady flow. As mentioned above, they observed that for the field-averaged transport, *D* increased with travel time to a depth of 3.0 m. However, in a later study with a similar water flow regime, Ellsworth and Jury (1991) used 13 small plots (2.25-4.0 m²) located throughout the same 0.64-ha field to study the three-dimensional transport of compact solute plumes. They used soil coring to sample the plots, three of which were sampled three times sequentially. For each plot, at each sampling time, horizontally integrated recoveries were well characterized by a "scaled" CDE with two constant, field-average fitting parameters indicating that the dispersivity did not increase with travel time.

Our study was designed to address some of the questions raised by the contrasting results of Butters and Jury (1989) and Ellsworth and Jury (1991). The different measurement devices used in these two studies seemingly resulted in quite different characterizations of solute transport. Thus, the objectives of our study were to: (i) examine the efficacy of two sampling techniques for characterizing solute transport under steady-state water flow, (ii) study the variation in transport model parameters with increasing depth of solute leaching, and (iii) perform model discrimination to examine the transport process operative within a field plot.

MATERIALS AND METHODS

Site Description

Our study was performed in a 2 by **2** m field plot located adjacent to the U.S. Salinity Laboratory in Riverside, CA. The soil is a Pachappa fine sandy loam (coarse-loamy, mixed,

thermic Mollic Haploxeralf). Steady-state ponded infiltration rates and unsaturated hydraulic properties were determined for the plot prior to this experiment, and the horizontal correlation scale of the deconvoluted point semivariogram for steady-state ponded infiltration was approximately 0.1 m (Shouse et al, 1994). Unsaturated hydraulic properties were estimated using the instantaneous profile method (Shouse et al, 1992). During the profile excavation at the completion of the solute transport study reported here, five bulk density samples using 7.62-cm-diam. cores were collected from within the 2 by 2 m plot for each 0. l-m layer to a depth of 2.0 m. In addition, the soil particle-size composition in 0.3-m increments was also measured to a depth of 1.95 m. The particle-size analysis is given in Table 1, which indicates some variation in textural composition with depth, especially the lower total coarse content (gravel + sand) and higher silt and clay contents between the 0.45 and 1.05-m depths. (The gravel, >2-mm fraction, was nearly all in the 2-3-mm size range.) The plot surface was prepared before the study using a hand-held rotary hoe to till the upper 0.03 m of the soil and level the plot surface. Foot traffic was confined to a portable "catwalk".

Instrumentation

We **used** a fully automated, high-uniformity (coefficient of uniformity X.95) water and solute applicator (Skaggs et al., 1990) with a 3.5-m spray boom on a 4.0-m track to maintain near-steady-state water flow conditions during the study. Water was applied to the plot every 0.5 h in a pulse of 2-min duration at an overall rate of 0.054 cm h^{-1}. A buffer area around the plot was maintained using trickle irrigation lines, which applied water at a rate similar to the sprayer. The entire area was enclosed with a 1.2-m-high wall covered with a greenhouse shade screen to minimize wind disturbance of the sprayer application.

Figure 1 shows a schematic diagram of the neutron probe access tube and tensiometer placements in the center of the plot. Measurements were taken every other day during the study to monitor the steady-state water content and potential conditions. These instruments had previously been used for the instantaneous profile method and had been in place for >2 yr. In addition, two arrays of 12 solution samplers (2.5-cm o.d. and 2.5-cm length porous ceramic cups, wall thickness of 0.3 cm) were installed at depths of 0.25 and 0.65 m. A slurry of diatomaceous earth was inserted into each hole prior to installing the suction lysimeters to ensure uniform contact between the cup and the surrounding soil. A suction of approximately 0.5 m was applied to each solution sampler at the same time each day for 10 min. This procedure provided about 20 mL of solution. We discarded the first 10 mL (the "dead" volume within the tubing and solution samplers) and analyzed the second 10 mL. A total of five drainable microlysimeters were installed on two opposite ends of the plot (Fig. 1) for

Table 1. Particle-size analysis and bulk density at the soil used in this study.

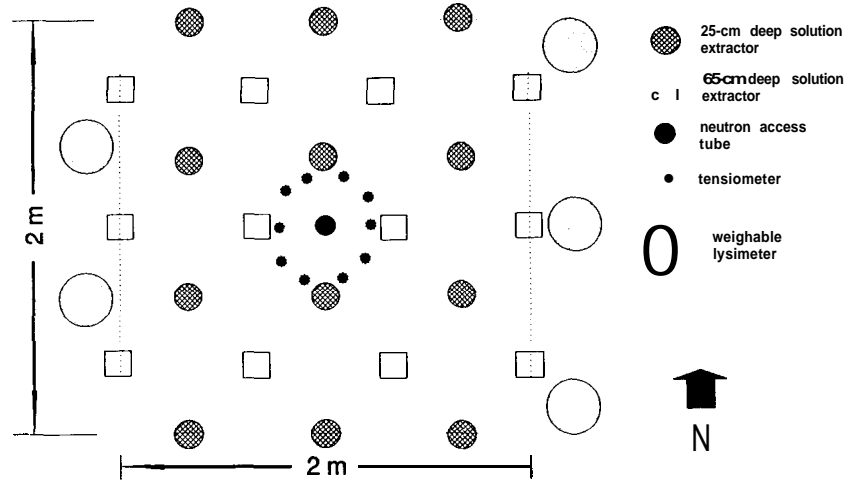| Depth interval	Gravel content (>2 mm)	Sand (2-0.05 mm)	silt (0.05-0.002 mm)	Clay (<0.002 mm)	Bulk density
cm			%		Mg m⁻³
o-15	9.6	40.2	42.1	7.5	1.67
15-30	10.5	38.2	43.8	7.5	1.68
30-45	18.8	36.3	37.6	7.3	1.75
45-75	13.5	28.7	45.3	12.5	1.73
75-105	11.0	21.5	50.8	10.7	1.58
105-135	19.1	24.5	46.9	9.5	1.71
135-165	36.5	21.4	35.3	6.8	1.83
165-195	17.9	34.2	46.7	1.2	1.79

Fig. 1. Plot layout, indicating location of small weighing lysimeters, 0.25 and 0.65m-deep solution samplers, tensiometers, and neutron probe access tube.

water balance measurements (0.2-m i.d., 0.25-m length) (Boast and Robertson, 1982). At each lysimeter location, the soil was removed from the plot, mixed, and repacked uniformly into the lysimeter. The surface of each lysimeter was flush with the surrounding soil surface. Two solution samplers were placed at the bottom of each lysimeter and subjected to continuous suction extraction using a suction approximately equal to that in the surrounding soil at the 0.25-m depth (measured by tensiometerj. The lysimeters were removed daily for weighing.

Solute Application

Tensiometer and neutron probe measurements showed that near-steady-state flow conditions within the plot were established during a 30-d pre-experiment water application. Prior to solute applications, soil cores were taken adjacent to the plot for determining background solute concentrations. Three iuorganic tracers, (Cl- [CaCl$_2$], NO$_3^-$ [Ca(NO$_3$)$_2$], and Br-[KBr]) were applied consecutively via the sprayer as illustrated in Fig. 2. Applied solute concentrations (157.8 g m^{-2} Cl-, 276.5 g m^{-2} NO$_3^-$, and 314.2 g m^{-2} Br$^-$) were at least three orders of magnitude higher than the measured background concentrations. The solute pulse duration was varied by an

order of magnitude among the tracers to facilitate dispersion model testing and to provide nearly equivalent vertical plume dimensions at the time of sampling. A transport model capable of describing all three pulses with the same parameter set would be considered a valid transport process description for the experimental conditions. A set of 28 cups placed adjacent to the 2 by 2 m study area was used to determine application uniformity and total solute mass applied.

Excavation

The plot was excavated during a 54-h period beginning 27 d and 27 cm of net applied water (NAW) after the first solute application. Each horizontal 0.1-m soil layer to a depth of 2.0 m was sectioned into 162 samples on a nested nine by nine grid as shown in Fig. 3. Each of the 81 cells yielded two samples (explained below). The surface elevation of each layer was measured using a theodolite survey instrument. A rigid steel blade attached to a cable pulley assembly and an angle iron support with guide were used to slice each layer.

The sampling design provided two measurement scales, a larger cell size of 22.2 by 22.2 by 10 cm and a smaller "core" sample of 7.4 by 7.4 by 10 cm. (The sample collected in the area surrounding the smaller core sample is called the donut sample.) The entire volume of soil to a depth of 2.0 m was thus completely removed. An additional 81, 7.62-cm-diam. soil cores were taken between a depth of 2.0 and 2.25 m and sectioned into two 0.125-m vertical increments. Chemical analysis of these cores established that tracer movement was limited to the upper 2.0 m of soil. All core samples were sealed in plastic bags and stored at 4°C until extracted. After thorough mixing, a 0.2-kg subsample was taken from each donut sample for gravimetric water content measurement. A 0.5-kg subsample was sealed in a plastic bag and stored at −10°C for extraction. The remainder of the sample was discarded.

Extraction and Analysis

Upon removal from cold storage, soil pastes were made using an approximate 2:1 water to soil ratio. After mixing and equilibrating, solution extracts were obtained using suction funnels lined with filter paper. Spiked soil standards were used to verify extraction efficiency and analytical methods. (Spiked soil standards were prepared by applying a known mass of
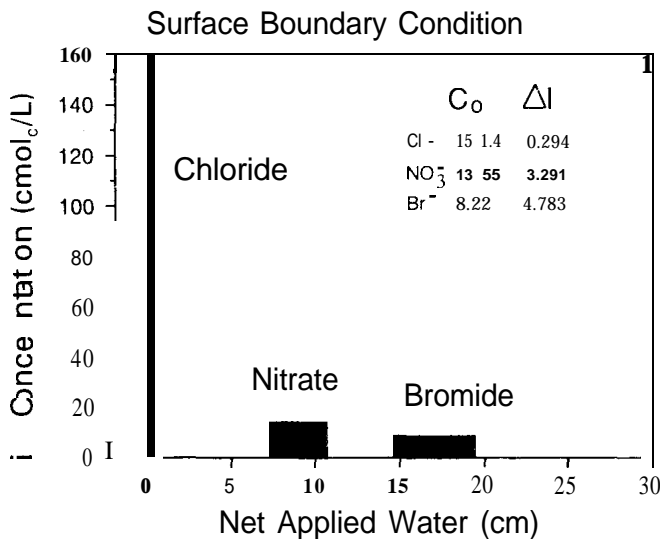

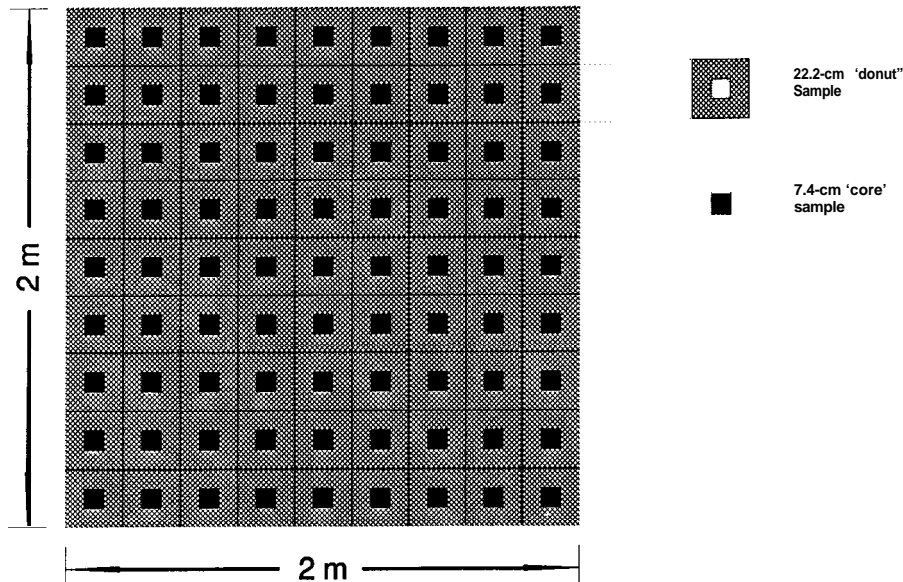**Fig. 2. Applied solute concentrations during near-steady-state water flow.**

Fig. 3. Sampling design for each 0.10-m layer to a depth of 2.0 m.

solute in solution to a specified mass of moist soil, followed by thoroughly mixing the sample. Solution extracts were then obtained from these spiked samples using the same extraction procedure as with the field study samples.) Chemical analyses for each tracer were performed in two separate laboratories for each sample extract. Analyses were repeated when measurements from the two labs did not agree within 6%. Chloride and Br- were determined by separate colorimetric methods, and Cl- plus Br was measured using a Ag titration procedure. Nitrate was determined using a colorimetric procedure on both automated segmented and continuous-flow analysis instruments. The chemical concentrations of the solution sampler extracts and the samples obtained daily from each lysimeter were determined likewise.

Data Analysis

Process Descriptions

Taylor (1953) discussed two distinct time scales of solute transport for laminar flow within a capillary tube. He described how the relation between these two time scales determined the form of the "global", or average, transport process within the tube. These two time scales were classified as a mean solute residence time scale (τ_r) and a characteristic transverse diffusion time scale (τ_D). Two limiting types of the flow process were identified. The first occurred when the mean residence time was much smaller than the transverse diffusion time scale ($\tau_D \gg \tau_r$). This resulted in what was termed convection-*dominated flow*. The second limiting type of flow occurred when $\tau_r \gg \tau_D$. For this situation, the transverse averaged solute concentration was shown to obey the CDE model with the mean solute velocity equal to the area-weighted mean flow velocity, and with the longitudinal spreading characterized by a constant "dispersion" coefficient that was a function of the flow properties.

Jury and Roth [1990] used an analogy between Taylor's analysis of laminar flow through a capillary tube and solute transport through "macroscopically" homogenous unsaturated soil to describe two contrasting field-scale processes. One of

these descriptions (analogous to $\tau_r \gg \tau_D$) gives the traditional CDE:

$$RV\frac{\partial C^f}{\partial t} = D\frac{\partial^2 C^f}{\partial z^2} \qquad \partial z \qquad [1]$$

where C^f is the flux concentration, R is the retardation factor, t is time, z is depth (positive downward), D is the dispersion-diffusion coefficient, and V is the velocity. When fitting the three parameters in Eq. [1] to data, only two can be independently estimated, for example V/R and DIR. The ratio D/V is called the dispersivity and is denoted a. For steady flow, the CDE process gives a travel-time variance (the variance of the BTC travel times) that increases linearly with mean travel time (Valocchi, 1985; Jury and Sposito; 1985).

The second stochastic process description, termed stochastic-convective (analogous to $\tau_D \gg \tau_r$), is defined in probabilistic terms by the relation $P(Z,t) = P(\lambda, t\lambda/Z)$, where λ is a reference calibration depth and P(Z,t) is the probability that a solute molecule entering the soil at time $t = 0$ has passed beyond depth Z during the time from $t = 0$ to $t = t$. For steady flow, a stochastic-convective process is typified by a travel-time variance that increases as the square of the mean travel time. In practice, a lognonnal travel time probability density function (pdf) is most often used to formulate this process description, which leads to the CLT model [Jury, 1982].

The CLT and CDE models for steady flow in a homogenous soil were used to analyze the transport process observed in our study. We used analytical solutions of constant-parameter CDE and CLT models to improve parameter identification, since we did not have reliable estimates of hydraulic property variations with depth. In addition, it appeared that such variations were minor: between the surface and the maximum depth of solute leaching, the steady-state volumetric water content varied from 27 to 33.5 %, suggesting a relatively uniform profile (in contrast to that observed in other studies, i.e., Roth et al., 1991; Butters and Jury, 1989; Ellsworth and Jury, 1991). Figure 4 gives the mean and 95% confidence levels for the sole profile volumetric water content (i) as measured with the neutron probe every other day during steady flow, and (ii) at the time of sampling, determined as the product of the mass-based water content (mean of 81 samples per layer)
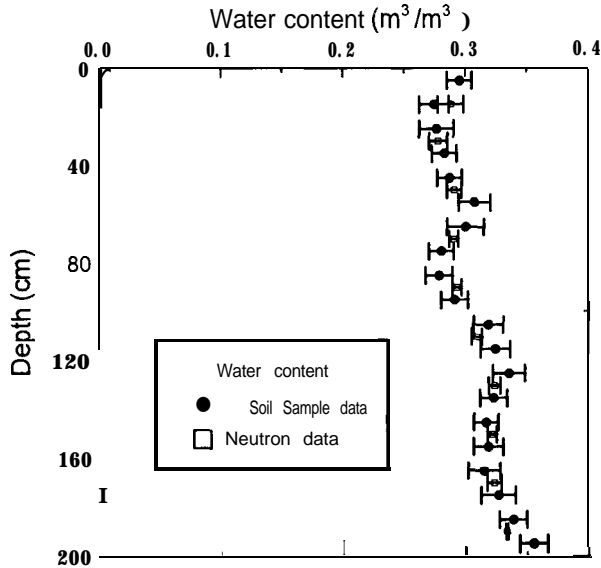
Fig. 4. Volumetric water content measured by (i) neutron probe during steady-state water application, and (ii) sampling at time of excavation.

Fig. 5. Cumulative net applied water, observed lysimeter drainage, and simulated drainage at 0.25 and 0.65-m depths.

and the bulk density (mean of five samples per layer). It is clear from this figure that variations in volumetric water content are greater in the vertical direction than within individual 0.1 -m layers. Presumably, variability in particle size and bulk density (porosity) are causing these variations in steady-state water content.

Prior to analysis, a fluid coordinate transform, identical to that of Ellsworth and Jury (1991), was used. This approach transformed the spatial depth coordinate into an equivalent "fluid" coordinate that represents the volume of water stored between the soil surface and the indicated depth. The time coordinate was transformed into a cumulative drainage coordinate (Wierenga, 1977; Jury et al., 1990). These transforms served two purposes. First, in fluid coordinates the volumetric water content is constant (and equal to unity) for all depths. Second, the cumulative drainage transformation changed minor variations in surface water flux with time into an effective constant "flux" rate, giving a mean pore water "velocity" in fluid coordinates constant with both depth and time (and equal to unity). A water content and mean pore water velocity that are constant with depth and time are consistent with the analytical solutions we used. Further, this approach also simplifies estimating the effective transport volume..

The cumulative drainage was estimated in two ways: from measured daily net applied water and from a flow simulation based on measured unsaturated hydraulic properties. These properties were found to be approximately the same as previously reported by Rooij (1989): saturated water content (θ_s) = 0.37; saturated hydraulic conductivity (K_s) = 2.0 cm h^{-1}; residual water content (θ_r) = 0.01; and (as fitting parameters in the van Genuchten model) a = 0.016 cm^{-1} and n = 1.67. These measured hydraulic properties were used with the HYDRUS (numerical solution of the one-dimensional Richards equation) code of Kool and Van Genuchten (1991) to estimate drainage fluxes in the soil profile. The simulated drainage at the time of each sample collection was used for the 0.25 and 0.65-m BTCs. In addition, since the sampling period occurred during a 54-h period and water application ceased at the start of the first day of sampling, the numerical simulation was used to estimate the cumulative drainage during the sampling period at the depth of the center of mass of each plume. The measured boundary and initial conditions were used in all
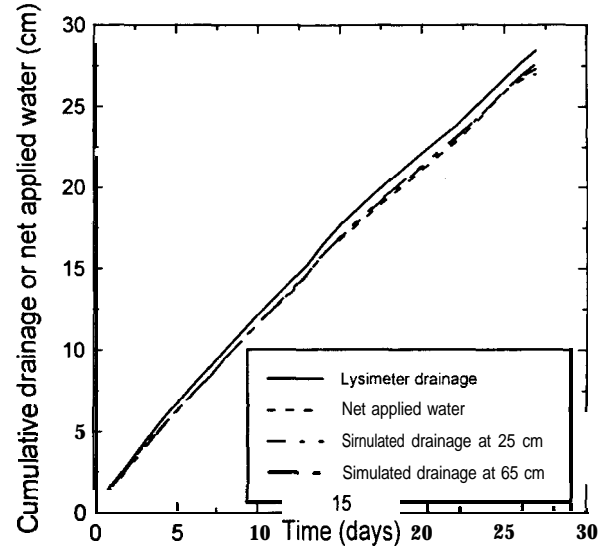
simulations (evaporation estimates obtained from weighing lysimeters).

Figure 5 shows the cumulative NAW vs. time. Also included are the cumulative average drainage from the five weighing lysimeters (0.25cm depth) and the HYDRUS-simulated drainage at depths of 0.25 and 0.65 m. The measured cumulative NAW and the HYDRUS-simulated drainage for both depths are quite similar. A linear regression (forced through the origin) of NAW vs. time yielded an average "steady-state" flux of 1.06 cm d^{-1} with a coefficient of determination of 0.99. However, there is a slight concave downward shape to these curves, indicating a decreasing daily NAW flux. Although the actual water application rate remained constant, it is evident that the average evaporation rate increased during the month of study (July). The average NAW flux was 1.21 cm d^{-1} for the first 6 d, 1.05 cm d^{-1} during the next 7 d, and 0.89 cm d^{-1} for the last 14 d. Despite this decreasing flux rate, we did not detect changes in volumetric water content (Fig. 4, neutron probe data) or hydraulic head (Fig. 6) during the study period. (Figure 6 shows the average hydraulic head profile measured every other day during steady flow. The linear relationship in this figure indicates an average hydraulic gradient of - 1.1 $(r^2$ = 0.96) for the study period.) The influence of this variable net application rate on parameter estimation is discussed below.

As noted by Kreft and Zuber (1978) and Parker and van Genuchten (1984a), the mode of detection must be considered when interpreting observations of solute transport. These researchers defined flux and spatial-weighted solute concentrations as flux and *resident concentrations,* respectively. Parker and van Genuchten (1984a) showed that if the flux (resident) concentration obeys Eq. [1], then the resident (flux) concentration *is* governed by the same equation and parameters. Therefore, expressing the experimental conditions in terms of the CDE gives:

$$C(x,0) = 0$$

$$-\omega D \frac{\partial C^i}{\partial z} + V C^i = \begin{bmatrix} V C_o & 0 < t \le \mathbf{A}t \\ 0 & t > \Delta t \end{bmatrix}$$

$$\frac{\partial C^i}{\partial z}(\infty, t) = 0 \qquad [2]$$
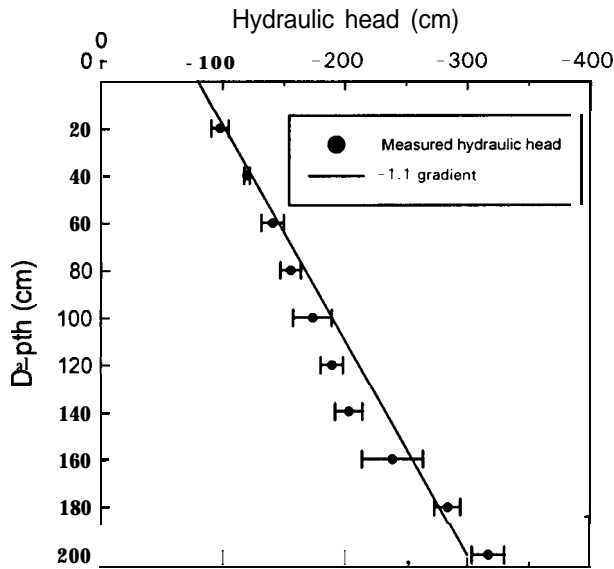
Hydraulic head (cm)

Fig. 6. Average hydraulic head for entire Row period (measured every other day).

where C_o is the applied solute concentration, At is the duration of solute application, and ω is equal to unity for resident (i = r) and 0 for flux (i = f) concentrations. The corresponding analytical solutions to Eq. [1] and [2] are given in van Genuchten and Alves (1982) as Eq. [A1] for flux and [A2] for resident concentrations. These solutions were used for obtaining CDE parameter estimates derived from the BTCs and depth profiles, respectively. (The measurements obtained from the direct excavation are considered resident concentrations, i.e., concentrations per unit volume of liquid phase. However, the assignment of a solution sampler measurement as either a flux or resident concentration is ambiguous. In our study we interpreted these measurements as flux concentrations. As pointed out by Parker and van Genuchten [1984a], the distinction between the two is not important for a convective-dispersive process with a small dispersivity.)

The CDE model parameters in the fluid coordinate system, V_m and D_m, varied slightly depending on whether we interpreted the solution sampler BTCs as flux or resident concentrations. Both V_m and D_m were consistently greater when BTCs were estimated as resident concentrations. For example, for the individual Cl- BTCs at 0.25 m, V_m averaged 3.8 % larger, and D_m 5.3 % larger. Variations in C_o were generally <0. 1%.

The CLT model analytical solution for a BTC, corresponding to Eq. [A1], is given as:

$$C^f(z,t) = \frac{C_o}{2}\left\{ 1 + \text{erf}\left[\frac{\ln\left(\frac{t\lambda}{t_u z}\right) - \mu_\lambda}{\sqrt{2}\sigma_\lambda} \right]\right\} \quad t \leq \Delta t$$

$$C^f(z,t) = \frac{C_o}{2}\left(\text{erf}\left[\frac{\ln\left(\frac{t\lambda}{t_u z}\right) - \mu_\lambda}{\sqrt{2}\sigma_\lambda} \right]\right.$$
$$\left. - \text{erf}\left\{ \frac{\ln\left[\frac{(t - \Delta t)\lambda}{t_u z}\right] - \mu_\lambda}{\sqrt{2}\sigma_\lambda} \right\}\right) \quad t > \Delta t \quad [3]$$

where C' denotes a flux concentration, t_u is a unit time (to provide that the logarithmic argument is unitless), μ_λ and σ_λ are CLT model parameters (Jury and Roth, 1990), and λ signifies an arbitrary depth to which all CLT parameter estimates, regardless of z, are referenced.

The CLT solution for a depth profile, corresponding to Eq. [A2], is:

$$C^r(z,t) = \frac{J_w C_o t_u}{2\lambda} \exp\left(\mu_\lambda + \frac{\sigma_\lambda^2}{2}\right)$$

$$\left\{ 1 + \text{erf}\left[\frac{\ln\left(\frac{t\lambda}{t_u z}\right) - \mu_\lambda - \sigma_\lambda^2}{\sqrt{2}\sigma_\lambda} \right]\right\} \quad \leq \Delta t$$

$$C^r(z,t) = \frac{J_w C_o t_u}{2\lambda} \exp\left(\mu_\lambda + \frac{\sigma_\lambda^2}{2}\right)$$

$$\left(\text{erf}\left[\frac{\ln\left(\frac{t\lambda}{t_u z}\right) - \mu_\lambda - \sigma_\lambda^2}{\sqrt{2}\sigma_\lambda} \right]\right.$$
$$\left. - \text{erf}\left\{ \frac{\ln\left[\frac{(t - \Delta t)\lambda}{t_u z}\right] - \mu_\lambda - \sigma_\lambda^2}{\sqrt{2}\sigma_\lambda} \right\}\right) \quad t > \Delta t$$

$$[4]$$

with C^r a resident solute concentration, and J_w the water flux density (L T^{-1}). (These solutions can be expressed in terms of cumulative drainage [I] by replacing t everywhere it appears in Eq. [3] and [4] with I and setting J_w equal to 1 and unitless.)

Parameter Estimation

Jury and Sposito (1985) discussed several methods for parameter estimation (i.e., MLE, SSQ, and MM) and defined two distinct types of error, the first being that the model process description differed from the true process, and the second that the number of observations did not adequately characterize the process within the spatial or temporal region under study. The measurements obtained from the total excavation are assumed to be free from the latter type of error, whereas this error would be present in the solution sampler BTCs and the smaller scale measurements. This is consistent with the close correspondence between the water content profile measured at the time of sampling and that estimated by neutron probe during flow, which suggests that relatively little drainage occurred during the 54-h sampling period. This is also supported by a one-dimensional water flow simulation that accounted for the observed evaporation and used the measured hydraulic properties for the site (HYDRUS, Kool and van Genuchten [1991]). A simulated drainage of 0.5, 0.4, and 0.1 cm occurred between the final water application and the time of sampling of the center of mass for Cl-, NO_3^-, and Br$^-$, which gave final estimates of I = 27.5, 20.1, and 12.5 cm, respectively.

The optimal parameter estimation method depends on the criteria used to define optimal. If one is concerned with predicting the concentration at any time or depth, a SSQ would be optimal in that it tries to minimize the deviation between

observed concentration values and model predictions, whereas a MM parameter estimation may be optimal if the concern is to predict groundwater contamination, since this method is more sensitive to extremes in the data.

We chose to use SSQ for parameter estimation, since one objective of the study was to quantify the vertical dispersion process. The SSQ method has the advantage of providing approximate CI about parameter estimates. As shown by Wagner and Gorelick (1986) and Knopman and Voss (1987), the agreement between these approximate CI and those generated by Monte Carlo analysis increases with decreasing random error. The CXTFIT code (Parker and van Genuchten, 1984b) was modified to include the CLT model (Eq. [2] and [3]), and the estimation of C_o. This allowed five parameters to be varied for the CDE model and four for the CLT. However, as mentioned above following Eq. [1] (see also discussion on p. 26-28 of Parker and van Genuchten [1984b]), not all of these parameters can be estimated simultaneously from observed data. We therefore arbitrarily set R equal to unity for the CDE and, for both models, fixed the pulse durations (expressed as cumulative drainage) to the actual values as given in Fig. 2. Thus, three parameters were optimized for each chemical for each model (i.e., C_o, V_m, and D_m for the CDE model; and C_o, μ_λ, and σ_λ for the CLT model) using data from the lysimeters, from the 0.25-m solution samplers, from the 0.65-m solution samplers, and from the concentration depth profiles (in fluid coordinates). For the CDE model, V_m plays the same role as V/R in Eq. [1]. Furthermore, when Eq. [1] is transformed into fluid coordinates, the fluid coordinate velocity parameter V_m (unitless) equals the real-space volumetric water content, $\theta_v(z)$, over the real-space effective transport volume, $\theta_e(z)$.

RESULTS AND DISCUSSION

Mass Balance

Table 2 is a summary of the applied and measured (by direct numerical integration and by an inverse method) solute mass for the 2 by 2 m plot area. Total mass of solute was estimated directly for each chemical by numerically integrating with time the average BTCs for the five lysimeters and for the 0.25- and 0.65-m solution samplers (following the procedure of Butters et al., 1989), and by numerically integrating with depth the concentration distribution as determined from the soil cores, the donut samples, and the weighted average of

the donut plus core samples. However, the final measured concentrations for the Br^- BTCs at 0.25 and 0.65 m, and the NO_3^- BTC at 0.65 m, did not allow direct mass estimates from numerical integration (see Fig. 7a and 7b). To supplement these calculations, an inverse method (Parker and van Genuchten, 1984b) was used to analyze the BTCs by fitting a solution of the CDE (Eq. [A1] of van Genuchten and Alves, [1982]) to the data.

Although a poorly defined measure of model fit for nonlinear models, the coefficients of determination, r^2, for fitted vs. measured data were generally >0.98. Figure 7a shows the model fit to the average BTCs for each tracer at the 0.25-m depth, and Fig. 7b for the 0.65-m depth. Both inverse and direct estimates of mass show that the solution samplers consistently underestimated the applied mass as did, to a lesser extent, the lysimeters. Based on inverse estimates, approximately 71% of the mass applied was recovered for the 0.25-m suction cups and 80% for the 0.65-m suction cups. Furthermore, for all of the average BTCs that were sufficiently complete, both direct and inverse estimates of mass recovery were less than applied. This trend is also evident with the individual BTCs: the inverse mass recovery estimates were less than applied for 53 of the 58 individual BTCs (one sampler at the 0.65-m depth malfunctioned). The consistency between the individual BTCs suggests that the poor performance of the solution samplers with respect to mass recovery is not attributable to a combination of spatial variability and too few measurements.

The solution samplers provide a measure of the solute concentration at the cup location in the soil, and not a measure of the soil water flux. Yet the solute mass flux is the product of the two. Thus, a discrepancy between

Table 2. Mass recovery summary.

	Chloride		Nitrate		Bromide	
Applied	631		1106		1257	
Measured	direct†	inverse‡	direct†	inverse‡	direct†	inverse‡
Lysimeter	608	544	976	942	1116	1171
0.25-m sampler	494	409	701	789	ID§	960
0.65-m sampler	449	494	ID§	914	ID5	ID5
Depth profile core	650	654	1067	1024	1260	1234
Depth profile donut	604	604	1155	1082	1329	1300
Depth profile total	609	610	1145	1076	1321	1294

† Data obtained from numerical integration of breakthrough curve.
‡ Estimate obtained as $C_oV_m\Delta I$, from convection-dispersion equation model fit of V_m and C_o to average breakthrough curve.
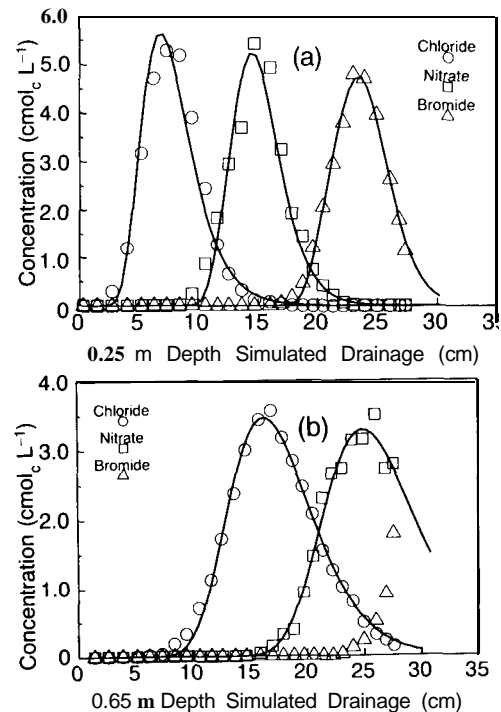§ Insufficient data for estimate.

Fig. 7. Convection-dispersion equation model fitted to the (a) 0.25-m-deep and (b) 0.65-m-deep solution sampler average breakthrough curve for each tracer using the least squares regression procedure.

the applied mass and that estimated from a BTC may be due to a covariance between the water flux and the solute concentration (this covariance would be at scales less than that corresponding to the BTC). An ideal solution sampler would sample the complete spectrum of solute flow paths, weighting the solute concentration in each path with the corresponding water flux, and thereby provide a representative flux concentration.

The five lysimeters also underestimated the mass applied, although to a lesser extent, only about 4 to 15%. The improved mass balance for the lysimeters relative to the solution samplers is probably a consequence of the forced one-dimensional flow and continuous sampling of the former. As expected, mass balance from the total direct excavation provided the best results, with a 96 to 105% recovery of applied mass for all three chemicals, and inclusion of the core samples widens the range only to 93 to 105%.

Table 3 contains the SSQ-estimated parameters for each tracer, for both the CDE and CLT models, for all six recovery methods. Jury and Roth [1990] stated (p. 42) that, "(The CLT) is virtually indistinguishable from the CDE model when the parameters of each model are optimized to each other or to a common data set at a given depth". This statement is given in the context of flux concentration solutions and does not hold for resident concentrations. This overlap is thus expected for the lysimeter and solution sampler BTCs, which are observations of concentration with time at a fixed depth. The close agreement in R^2 values for the CDE and CLT in Table 3 for the lysimeter and solution sampler BTCs reflects this result. However, this overlap is not expected for model fits to observations of concentration vs. depth at a fixed time, as reflected by the greater discrepancy between CDE and CLT R^2 values for the depth profiles, with the latter model generally providing a better fit to the data. The optimized values of C_o for the depth profiles are a measure of mass recovery. The inverse estimated mass recovery in Table 2 was calculated from the CDE parameters in Table 3 as $V_m C_o \Delta l$ (cmol$_c$ L^{-1}), where AI is given in Fig. 2.

Mean Transport and Longitudinal Dispersion

Water flow within the soil profile deviated from steady state, as is evident by the decreasing NAW flux from 1.21 cm d^{-1} during the first week to 0.89 cm d^{-1} during the final 14 d of the study. The neutron probe measurements showed that this decreasing flux rate did not significantly decrease the average volumetric water content during the study. The hydraulic head measurements also did not reflect significant changes. (The accuracy of the neutron probe and tensiometer measurements are reflected in the 95% confidence bands about the data, Fig. 4 and 6, respectively.) Jury and Roth (1990, p. 202) showed that for θ_v constant and a $V = D$ = constant, all steady-flow CDE solutions are identical when plotted as a function of cumulative drainage, regardless of the magnitude of the water flux. A more general relation was given for flux-weighted concentrations by Barry

Table 3. Parameter estimates for convection-dispersion equation (CDE) and convective lognormal transfer function (CLT) models.

	Depth†	CDE				CLT			
		C_o‡	V_m	D_m§	r^2	C_o‡	μ_λ¶	σ_λ¶	r^2
	cm	cmol$_c$ L^{-1}	cm^3 cm^{-3}	cm		cmol$_c$ L^{-1}			
				Lysimeter#					
Cl$^-$	7.3	147.4	0.886	0.435	0.942	148.1	2.063	0.359	0.946
NO$_3^-$	7.3	12.0	0.965	0.391	0.975	12.2	1.972	0.323	0.976
Br$^-$	7.3	7.4	1.041	0.372	0.986	7.4	1.898	0.304	0.988
				0.25-m solution sampler					
Cl-	7.3	104.2	0.944	0.336	0.989	106.7	2.041	0.306	0.989
NO$_3^-$	7.3	8.2	1.175	0.448	0.967	8.7	1.812	0.327	0.967
Br-	7.3	5.8	1.086	0.315	0.992	5.8	1.862	0.279	0.993
				0.65-m solution sampler					
Cl-	18.9	109.3	1.085	0.515	0.995	109.5	1.878	0.223	0.996
NO$_3^-$	18.9	10.3	1.086	0.620	0.990	10.3	1.871	0.242	0.990
				Core sampling					
Cl-	34.3	129.5	1.213	0.945	0.993	158.4	1.758	0.213	0.990
NO$_3^-$	23.8	10.1	1.246	0.778	0.972	12.6	1.723	0.222	0.984
Br-	13.5	6.4	1.261	0.400	0.993	8.2	1.716	0.222	0.999
				Donut sampling					
Cl-	34.5	120.4	1.206	0.918	0.990	147.1	1.764	0.212	0.997
NO$_3^-$	23.4	10.9	1.213	0.594	0.975	13.4	1.754	0.204	0.988
Br-	13.2	6.9	1.236	0.411	0.993	8.6	1.733	0.227	0.999
				Total values					
Cl-	34.5	121.4	1.207	0.922	0.990	148.4	1.763	0.212	0.997
NO$_3^-$	23.4	10.8	1.216	0.613	0.975	13.3	1.751	0.206	0.988
Br-	13.2	6.8	1.239	0.411	0.993	8.6	1.731	0.227	0.999

† Fluid coordinate depth (plume center of mass for core, donut, and total).
‡ C_o gives an estimate of mass applied (meq cm^{-2}) as: $V_m C_o \Delta l/1000$ (for CDE) and $C_o \Delta l/1000$ (for CLT).
§ V_m is equal to θ_v/θ_e and is assumed to be constant with depth, D_m has units of centimeters in fluid coordinate depth.
# CLT reference depth was 7.3 cm (fluid coordinates).
¶ The lysimeters represent repacked soil columns of 0.25-m length.

and Sposito (1989), who showed that using cumulative drainage in Eq. [A1] of van Genuchten and Alves (1982) will give the identical result as employing a solution for a variable flux, $q(r)$, with variable $V(t)$ and $\alpha V(t) = D(t)$.

We verified that Eq. **[A2]** in terms of cumulative drainage gives the same profile distribution for CDE resident concentrations with $\alpha V(t) = D(t)$ using an iterated integral Green's function solution. Briefly, Eq. [A2] was used to simulate 6 d of flow with $q_1 = 1.21$ cm d^{-1}. The resulting solute distribution, $C_1(z,t = 6d)$, was the initial condition in a Green's function solution with $q_2 = 1.05$ cm d^{-1} for the subsequent 7 d (the corresponding Green's function is given in Ellsworth and Jury, 1991). Then, in a final Green's function solution, the solute distribution at $t = 27$ d was calculated, with $C_2(z,t = 13d)$ as the initial condition, using $q_3 = 0.89$ cm d^{-1} for the final 14 d. This iterated integral approach gave identical parameter estimates, within four significant figures, as using Eq. **[A2]** directly with cumulative drainage instead of time. We thus used the relation $\alpha V_m = D_m$ in our CDE parameter estimates.

Mean Transport

As stated above, the V_m estimates in Table 3 are the ratio of volumetric water content to the effective transport volume, θ_v/θ_e. The total depth profile estimate of V_m for all three chemicals (approximately 1.22) corresponds closely to the relative velocities observed by Jaynes and Rice (1993) under drip irrigation and to 1/R for Cl^- and Br^- (R values between 0.8 and 0.83) reported by Porro et al. (1993). Table 3 shows that the V_m parameter estimates for the average lysimeter and solution sampler BTCs were consistently smaller than for the depth profiles (15% smaller on average). The estimated V_m for 48 of the 58 individual BTCs was less than the average depth profile V_m. These 58 BTC V_m estimates were approximately normally distributed, with the differences between the mean BTC and depth profile V_m estimates being significant at the 0.01 level. The CLT parameter estimates also differ between measurement methods, for instance the mean travel tune, μ_λ, is about 10% larger on average for the lysimeters and solution samplers than for the depth profile. Since the effect of a given percentage change in μ_λ has a different impact on solute transport predictions than the same percentage change in V_m, a direct comparison of relative parameter variations between CDE and CLT models is not appropriate.

In order to study variations in V_m and μ_λ on a common basis (and variations in D_m and σ_λ), each of the solution sampler and total depth profile parameter sets given in Table 3 were used to predict the vertical center of mass and variance of a hypothetical plume resulting from a finite solute application pulse of AI = 0.294, sampled after $I = 27.5$ cm. These predictions are shown in Fig. 8a and 8b, plotted against cumulative drainage at calibration (I_c). For the simulations that were run using parameters estimated from depth profile measurements, I_c is the cumulative drainage from the beginning of pulse application to sampling. For the simulations using
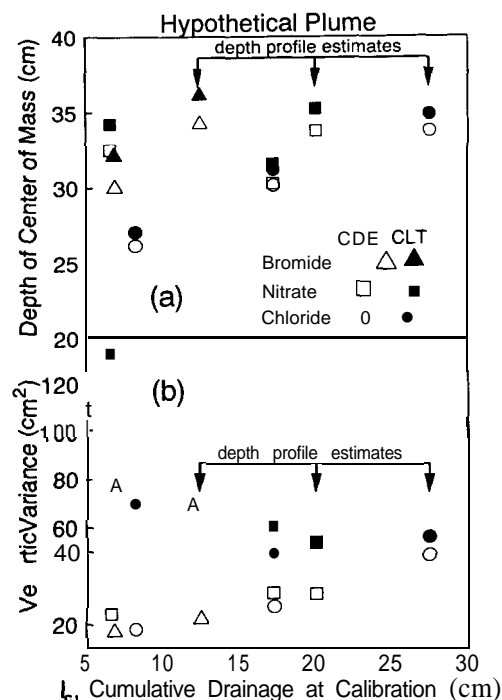

Fig. 8. Prediction of hypothetical plume (AI = 0.294, I = 27.5 cm): (a) depth of center of mass and (b) vertical variance, from solution sampler and total depth profile parameter estimates as given in Table 3.

parameters estimated from BTC data, I_c is the value of cumulative drainage corresponding to the average travel time of the BTC. The AZ and I used in these simulations were chosen to match the Cl^- plume (center of mass of 34.5 cm and a vertical variance of 49.5 cm^2, as determined from numerical integration with depth).

In Fig. 8a, the depth of the predicted center of mass is consistently less with the solution sampler data than the depth profile data, for both the CDE and CLT models. This suggests that the discrepancy between the studies of Butters and Jury (1989) and Ellsworth and Jury (199 1) at the same field site under similar flow conditions is partially a consequence of the sampling techniques used in those studies. (In this earlier work, estimates of mean solute velocity from solution samplers [Butters and Jury, 1989] were significantly less than those observed by soil coring [Ellsworth and Jury, 1991].)

Note that the CLT model results in a consistently greater estimate of the mean depth of leaching. This may be a consequence of the skewed nature of the lognormal travel time pdf. The discrepancy between the CDE- and CLT-predicted center of mass decreases slightly with calibration time. This is either a consequence of less cumulative drainage between calibration time and time of prediction ($27.5 - I_c$) or it is due to a decrease in V_m and μ_λ parameter uncertainty with increasing I_c. As pointed out by Knopman and Voss (1987) for BTC data, CDE velocity parameter uncertainty decreases with increasing calibration distance from the solute source and this relationship can also be shown for the CLT model.

Table 4. Simultaneous least squares regression fit of convection-dispersion equation and convective lognormal transfer models to depth profile data with applied solute concentration (C_o) given from applied mass.

Depth profile used	CDE			CLT		
	V_m†	D_m†	RMSE‡	μ_λ	σ_λ	RMSE‡
	cm^3 cm^{-3}	c m	cmol$_c$ L^{-1}			cmol$_c$ L^{-1}
Br$^-$	1.24	0.39	0.124	1.74	0.22	0.068
Br- + NO,	1.22	0.52	0.201	1.74	0.21	0.114
Br- + NO$_3^-$ + Cl$^-$	1.22	0.65	0.223	1.74	0.21	0.104

† V_m *is* equal to θ_v/θ_e and is assumed to be constant with depth, D_m has units of centimeters in fluid coordinate depth.

‡ Root mean square error from regression.

Longitudinal Dispersion

The open symbols in Fig. 8b show a nearly linear increase in variance with I_c. This suggests an increasing D_m with mean residence time, or cumulative drainage. This can be seen in Table 3 as well. Since V_m was relatively constant, at least for the depth profile data, this gives a dispersivity, a, that increases with travel time. In Fig. 8b, the CLT-estimated vertical variance initially decreases with calibration time and then appears to stabilize after about 15 cm of cumulative drainage. This stability suggests that the CLT more closely characterizes the transport process than the CDE model, as is examined further below.

Model Discrimination

Since the total depth profile data excluded errors associated with incomplete sampling, we used these data to determine which model provided the best description of solute transport within the plot. Setting C_o equal to the applied mass for each tracer, we used a sequential parameter estimation method to examine the stability in parameter estimates and in RMSE with increasing observations.

These calculations, summarized in Table 4, show that the CLT provides a distinctly better description of the plot-scale transport process. Specifically, the CDE model D_m increases with increasing observations, while in the CLT model both parameters μ_λ and σ_λ remain stable. The RMSE for each of the three data sets is roughly twice as large for the CDE as for the CLT. In addition, the CDE RMSE increases monotonically with increasing observations, whereas the CLT RMSE decreases between the Br$^-$ + NO$_3^-$ fit and the Br$^-$ + NO$_3^-$ + CL- fit. The more accurate representation of the data by the CLT model is illustrated in Fig. 9. This figure compares the observed data with that estimated by the two models, each with two calibrated parameters (from simultaneous SSQ fitting to all three depth profiles) and with C_o given from the applied mass.

It is straightforward to relate the parameter estimates in Tables 3 and 4 for fluid coordinates to real space. In this study, variations in volumetric water content to a depth of 150 cm were minor; thus a depth-averaged water content can be used to transform the CDE parameters to real space. The CDE model parameters estimated in the fluid coordinates, V_m and D_m would scale as $V_z = J_w V_m/\theta_v$ and $D_z = J_w D_m/\theta_v^2$ (where V_z and D_z are equal to
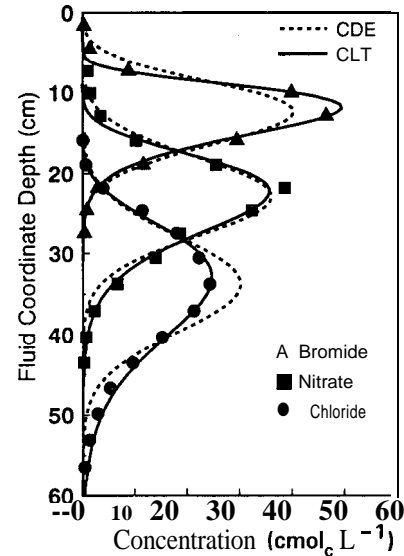

Fig. 9. The convection-dispersion equation and convective lognormal transfer function models, each fitted to the three depth profiles simultaneously, with applied solute concentration (C_o) equal to the applied mass (parameters given in bottom line of Table 4).

V/R and D/R of Eq. [1], respectively). Since the reference depth scales as well, the CLT μ_λ and σ_λ parameters are the same in either reference frame. These four transformations are all exact except for the depth profile V_m and D_m transformations, which are nearly so.

CONCLUSIONS

Intensive field studies of solute transport through unsaturated soil are limited because of the expense and time required. Thus, considerable uncertainty exists concerning the most appropriate process description in a given modeling situation. This study was performed to examine the efficacy of two sampling techniques for monitoring transport through unsaturated soil, to determine transport model parameter scale dependence, and to characterize the transport process at a plot scale. We showed that solution samplers consistently underestimate the mean solute velocity and applied mass, compared with soil samples. However, solution samplers did provide a reasonable description of vertical dispersion. Since solution samplers provide an inexpensive, rapid alternative for monitoring transport, the reasonable estimate of dispersion that they provide is promising. Further research is needed to examine the effect of solution sampler size, relative suction gradient, and frequency of extraction on the characterization of the underlying transport process.

Although an increasing dispersivity with travel distance is generally observed in aquifers (Gelhar et al., 1992), no such clear trend exists for the unsaturated zone (Porro et al., 1993). In this study, we observed a nearly linear increase in dispersivity with travel distance (maximum depth of solute leaching of 1.7 m). This transport process was also reflected by the greater stability in CLT parameter estimates with increasing observations and the twofold smaller RMSE for this model than for the CDE (based on the simultaneous two-parameter fit to the depth profiles for the three solutes), with the

former providing an excellent description of the plot-scale transport. It appears that the experimental method of applying different tracers by means of a series of pulses, coupled with different measurement methods, provides a valuable tool for process and parameter identification.

REFERENCES

Adams,E.E., and L.W. Gelhar. 1992. Field study of dispersion in a heterogeneous aquifer: 2. Spatial moments analysis. Water Resour. Res. 28:3293-3307.

Barry, D.A., and G. Sposito. 1989. Analytical solution of a convection-dispersion model with time-dependent transport coefficients. Water Resour. Res. 25:2407-2416..

Beven. K.J.. D.E. Henderson. and A.D. Reeves. 1993. Dispersion parameters for undisturbed partially saturated soil. J. Hydrol. (Amsterdam) 143: 19-43.

Biggar, J.W., and D.R. Nielsen. 1976. Spatial variability of the leaching characteristics of a field soil. Water Resour. Res. 12:78-84.

Boast, C. W., and T.M. Robertson. 1982. A "micro-lysimeter" method for determining evaporation from bare soil: Description and laboratory evaluation. Soil Sci. Soc. Am. J. 46:689-696.

Butters, G.L., and W.A. Jury. 1989. Field scale transport of bromide in an unsaturated soil. 2. Dispersion modeling. Water Resour. Res. 25:1583-1598.

Butters, G.L., W.A. Jury, and F.F. Ernst. 1989. Field scale transport of bromide in an unsaturated soil. 1. Experimental methodology and results. Water Resour. Res. 25:1575-1581.

Dagan, G. 1984. Solute transport in heterogeneous porous formations. J. Fluid Mech. 145:151-177.

Dagan, G. 1986. Statistical theory of groundwater flow and transport. Water Resour. Res. 22: 120s-134s.

Dagan, G. 1987. Theory of solute transport by groundwater. Annu. Rev. Fluid Mech. 19:183-215.

de Rooij, G.H. 1989. A numerical model for water and solute movement in a cropped soil profile. Res. Rep., Dep. of Soil Science and Plant Nutr., Agricultural Univ., Wageningen, the Netherlands. U.S. Salinity Lab., Riverside, CA.

Ellsworth, T.R., and W.A. Jury. 1991. A three-dimensional field study of solute transport through unsaturated, layered, porous media: 2. Characterization of vertical dispersion. Water Resour. Res. 27:967-981.

Gelhar, L.W., and C. Axness. 1983. Three-dimensional analysis of macrodispersion in aquifers. Water Resour. Res. 19: 161-180.

Gelhar, L.W., C. Welty, and K.R. Rehfeldt. 1992. A critical view of data on field-scale dispersion in aquifers. Water Resour. Res. 28: 1955-1974.

Hamlen, C.J., and R.G. Kachanoski. 1992. Field solute transport across a soil horizon boundary. Soil Sci. Soc. Am. J. 56:1716-1720.

Jaynes, D.B., and R.C. Rice. 1993. Transport of solutes as affected by irrigation method. Soil Sci. Soc. Am. J. 57:1348-1353.

Jury, W.A. 1982. Simulation of solute transport using a transfer function model. Water Resour. Res. 18:363-368.

Jury. W. A., J.S. Dyson, and G.L. Butters. 1990. A transfer function model of field scale solute transport under transient water flow. Soil Sci. Soc. Am. J. 54:327-331.

Jury, W.A., and H. Flühler. 1992. Transport of chemicals through soil: Mechanisms, models and field applications. Adv. Agron. 47: 141-201.

Jury, W.A., and K. Roth. 1990. Transfer functions and solute movement through soil: Theory and applications. Birkhauser Verlag, Basel, Switzerland.

Jury, W.A., and G. Sposito. 1985. Field calibration and validation of solute transport for the unsaturated zone. Soil Sci. Soc. Am. J. 49: 1331-1341.

Khan, A.U.H., and W.A. Jury. 1990. A laboratory test of the dispersion scale effect. J. Contam. Hydrol. 5:119-132.

Knopman, D.S., and C.I. Voss. 1987. Behavior of sensitivities in the one-dimensional advection-dispersion equation: Implications for parameter estimation and sampling design. Water Resour. Res. 23:253-272.

Kool, J.B., and M.Th. van Genuchten. 1991. HYDRUS, one-dimensional variably saturated flow and transport model, including hysteresis and root water uptake. Version 3.31. Res. Rep. no. 124. U.S. Salinity Lab., Riverside, CA.

Kreft, A., and A. Zuber. 1978. On the physical meaning of the dispersion equation and its solutions for different initial and boundary conditions. Chem. Eng. Sci. 33:1471-1480.

Parker, J.C., and M.Th. Van Genuchten. 1984a. Flux-averaged and volume-averaged concentrations in continuum approaches to solute transport. Water Resour. Res. 20:866-872.

Parker, J.C., and M.Th. van Genuchten. 1984b. Determining transport parameters from laboratory and field tracer experiments. Bull. 84-3. Virg. Agric. Exp. Stn., Blacksburg.

Porro, I., P.J. Wierenga, and R.G. Hills. 1993. Solute transport through large uniform and layered soil columns. Water Resour. Res. 29:1321-1330.

Roth, K., W.A. Jury, H. Flühler, and W. Attinger. 1991. Transport of chloride through an unsaturated field soil. Water Resour. Res. 27:2533-2541.

Russo, D., 1991. Stochastic analysis of simulated vadose zone solute transport in a vertical cross-section of heterogeneous soil during non-steady water flow. Water Resour. Res. 27:267-283.

Russo, D., and G. Dagan. 1991. On solute transport in a heterogeneous porous formation under saturated and unsaturated water flows. Water Resour. Res. 27:285-292.

Shouse. P.J.. T.R. Ellsworth. and J.A. Jobes. 1994. Steady-state infiltration'as a function of measurement scale. Soil Sci. 157: 129-136.

Shouse, P.J., J.B. Sisson, T.R. Ellsworth, and J.A. Jobes. 1992. Estimating in situ unsaturated hydraulic properties of vertically heterogeneous soils. Soil Sci. Soc. Am. J. 56:1673-1679.

Skaggs, T.H., T.R. Ellsworth, and P.J. Shouse. 1990. An automated, high uniformity irrigation system for simulating arbitrary boundary conditions on small plots. p. 219. In Agronomy abstracts. ASA, Madison, WI.

Sposito, G., and D.A. Barry. 1987. On the Dagan model of solute transport through groundwater: Foundational aspects. Water Resour. Res. 23: 1867-1875.

Taylor, G.I. 1953. The dispersion of matter in solvent flowing slowly through a tube. Proc. R. Soc. London, Ser. A 219:189-203.

Valocchi, A.J. 1985. Validity of the local equilibrium assumption for modeling sorbing solute transport through homogeneous soils. Water Resour. Res. 21:808-820.

van Genuchten, M.Th., and W.J. Alves. 1982. Analytical solutions of the one-dimensional convective-dispersive solute transport equation. USDA Tech. Bull. 1661. U.S. Gov. Print. Office, Washington, DC.

van Genuchten, M.Th., and P.J. Shouse. 1989. Solute transport in heterogenous field soils. p. 177-187. In D.T. Allen, et al. (ed.) Intermedia pollutant transport. Plenum Publ. Corp., New York.

van Wesenbeeck, I.J. 1993. Horizontal spatial scale dependence of vertical solute transport. PhD. diss. Univ. of Guelph, Ontario, Canada.

Wagner, B.J., and S.M. Gorelick. 1986. A statistical methodology for estimating transport parameters: Theory and applications to one-dimensional advective-dispersive systems. Water Resour. Res. 22:1303-1315.

Wierenga, P.J. 1977. Solute distribution profiles with steady-state and transient water movement models. Soil Sci. Soc. Am. J. 41: 1050-1055.

Wierenga, P.J., and M.Th. van Genuchten. 1989. Solute transport through small and large unsaturated soil columns. Ground Water 27:35-42.